



Effects of Elevated CO₂ on a Natural Diatom Community in the Subtropical NE Atlantic

Lennart T. Bach^{1*}, Nauzet Hernández-Hernández², Jan Taucher¹, Carsten Spisla¹, Claudia Sforna¹, Ulf Riebesell¹ and Javier Aristegui²

¹ Biological Oceanography, GEOMAR Helmholtz Centre of Ocean Research Kiel, Kiel, Germany, ² Instituto de Oceanografía y Cambio Global, Universidad de Las Palmas de Gran Canaria, Las Palmas, Spain

OPEN ACCESS

Edited by:

Laura Anne Bristow,
University of Southern Denmark,
Denmark

Reviewed by:

Koji Suzuki,
Hokkaido University, Japan
Alex J. Poulton,
The Lyell Centre, United Kingdom

*Correspondence:

Lennart T. Bach
lbach@geomar.de

Specialty section:

This article was submitted to
Marine Biogeochemistry,
a section of the journal
Frontiers in Marine Science

Received: 31 October 2018

Accepted: 11 February 2019

Published: 01 March 2019

Citation:

Bach LT, Hernández-Hernández N, Taucher J, Spisla C, Sforna C, Riebesell U and Aristegui J (2019) Effects of Elevated CO₂ on a Natural Diatom Community in the Subtropical NE Atlantic. *Front. Mar. Sci.* 6:75. doi: 10.3389/fmars.2019.00075

Diatoms are silicifying phytoplankton contributing about one quarter to primary production on Earth. Ocean acidification (OA) could alter the competitiveness of diatoms relative to other taxa and/or lead to shifts among diatom species. In spring 2016, we set up a plankton community experiment at the coast of Gran Canaria (Canary Islands, Spain) to investigate the response of subtropical diatom assemblages to elevated seawater $p\text{CO}_2$. Therefore, natural plankton communities were enclosed for 32 days in *in situ* mesocosms ($\sim 8 \text{ m}^3$ volume) with a $p\text{CO}_2$ gradient ranging from 380 to 1140 μatm . Halfway through the study we added nutrients to all mesocosms (N, P, Si) to simulate injections through eddy-induced upwelling which frequently occurs in the region. We found that the total diatom biomass remained unaffected during oligotrophic conditions but was significantly positively affected by high CO₂ after nutrient enrichment. The average cell volume and carbon content of the diatom community increased with CO₂. CO₂ effects on diatom biomass and species composition were weak during oligotrophic conditions but became quite strong above $\sim 620 \mu\text{atm}$ after the nutrient enrichment. We hypothesize that the proliferation of diatoms under high CO₂ may have been caused by a fertilization effect on photosynthesis in combination with reduced grazing pressure. Our results suggest that OA in the subtropics may strengthen the competitiveness of (large) diatoms and cause changes in diatom community composition, mostly under conditions when nutrients are injected into oligotrophic systems.

Keywords: ocean acidification, climate change, mesocosm, food web, phytoplankton, Bacillariophyceae

INTRODUCTION

Diatoms are a group of globally distributed phytoplankton, with an estimated contribution of $\sim 25\%$ to global primary production (Nelson et al., 1995; Field et al., 1998; Tréguer and De La Rocha, 2013). All diatom species share the trait of protecting the organic part of the cell with a shell (frustule) made of amorphous silica (opal), probably to reduce grazing pressure (Hamm and Smetacek, 2007; Pondaven et al., 2007; Friedrichs et al., 2013; Liu et al., 2016). To form the frustule, diatoms require dissolved silicate as an additional nutrient, which is often limiting in seawater and hence limiting their proliferation (Brzezinski and Nelson, 1996). Diatoms are strong competitors

and typically dominate phytoplankton communities early in the succession when nutrients are sufficiently available (Sarthou et al., 2005).

There are at least 30,000 extant diatom species which span a size range from under 3 micro- up to a few millimeters (Mann and Vanormelingen, 2013). They occur as single cells or cell chains in benthic and/or pelagic habitats, and have free-living, surface-associated, symbiotic, or parasitic lifestyles (Armbrust, 2009; Mann and Vanormelingen, 2013).

Changes in diatom community composition can reorganize the flux of elements in oceans and the flow of energy within food webs (Armbrust, 2009; Tréguer et al., 2018). For example, particulate organic carbon sequestration to the deep ocean was shown to be 1.8 times higher in 1989 when the North Atlantic spring bloom was dominated by a larger species compared to the following year when smaller ones dominated (Boyd and Newton, 1995). Likewise, energy transfer to higher trophic levels is likely to be more efficient in assemblages where primary production is dominated by larger diatoms since less trophic intermediates are involved (Sommer et al., 2002). Thus, it is essential to determine how diatom community composition could be affected by different environmental stressors and in different ocean regions due to their enormous relevance for the Earth system.

In the present study we investigated how ocean acidification (OA) – the anthropogenic perturbation of seawater carbonate chemistry – could affect the composition of natural diatom communities in the subtropical NE Atlantic. Therefore, we set up a mesocosm experiment at the coast of Gran Canaria and perturbed the enclosed plankton communities with different CO₂ concentrations. In the study region, diatom blooms often occur in association with meso-/sub-mesoscale structures such as upwelling filaments, zonal fronts, or eddies which inject nutrients into the euphotic zone (Barton et al., 1998; Arístegui et al., 2004; McGillicuddy et al., 2007; Anabalón et al., 2014). To account for this, the mesocosms were enriched with inorganic nutrients (N, P, Si) halfway through the experiment. This allowed us to investigate CO₂ effects on diatoms during oligotrophic conditions (phase I) and during a subsequent nutrient injection to the euphotic zone (phase II).

MATERIALS AND METHODS

Mesocosm Design, Deployment, and Maintenance

On February 23, 2016, we deployed eight *in situ* mesocosms (M1–M8) at the pier of Taliarte harbor, on the eastern coast of Gran Canaria (Canary Islands, 27° 59' 24" N, 15° 22' 8" W). The cylindrical mesocosm bags (Ø 2 m, 2.5 m long) were made of transparent polyurethane foil (PU), which is also used for the larger version of the KOSMOS mesocosm design (Riebesell et al., 2013). The PU bags were installed in a floatation frame made of polyethylene with steel reinforcements and deployed inside the harbor (Figure 1). The floatation

frame was fixed on the pier and on mooring weights on the water side. A pulley system attached to the mooring weights allowed us to move the entire structure ~2 m away from the pier in between samplings. This was necessary to reduce the influence of the pier on the light environment inside the mesocosms.

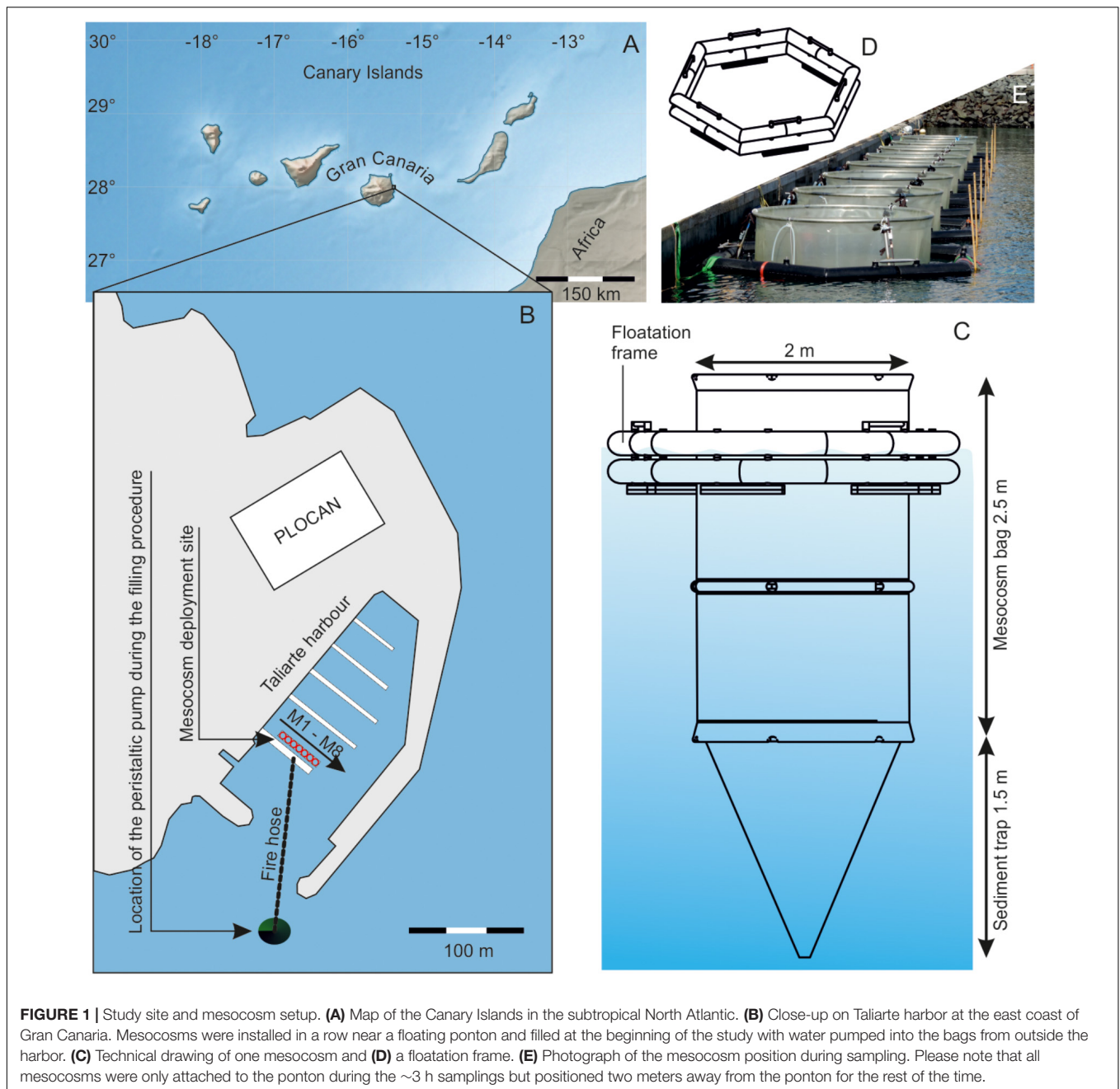
Conical sediment traps were attached to the bottom of the bags, thereby creating 8 isolated volumes (Figure 1). The sediment traps were 1.5 m long and similar to the KOSMOS design (Boxhammer et al., 2016). The mesocosms were initially empty and filled in the morning of March 2 by pumping seawater from ~30 m outside Taliarte harbor into the enclosures (Figure 1). Seawater was pumped with a peristaltic pump from 3 to 5 m depth through a hose (Ø 50 mm with a 3000 µm mesh attached to the inlet) into a central volume on the pier, from where the seawater was simultaneously distributed with separate hoses (Ø 37 mm) into the mesocosms. The entire filling procedure lasted ~4.5 h, and we tried to keep the stress level for pumped organisms low by restricting the speed of the peristaltic pump (3.9 L/s). We cannot fully ensure, however, that particularly sensitive organisms weren't harmed and excluded from the experiment. Each mesocosm contained a volume of ~8 m³ after filling. The filling marks the beginning of the experiment and is hereafter referred to as day -3, while day 0 is the day when the CO₂ manipulation started (see section "Experimental Design").

The mesocosm PU foil must be cleaned on a regular basis to avoid the growth of benthic organisms and to maintain light transmission. The outer sides of the mesocosm bags were cleaned by divers with brushes on days 6, 14, 17, and 25. The inner sides were cleaned on days 6, 14, 18, and 25 with a custom made cleaning ring which has approximately the same diameter as the mesocosm bags and thoroughly wipes the foil while sliding downward (Riebesell et al., 2013). The sediment traps were cleaned from the inside on day 15 with custom made "magnetic brushes" since the cleaning ring could not reach this part of the mesocosms. The magnetic brushes are basically two brushes that connect through the PU foil with a magnet and are operated from the outside by divers.

M1 was damaged early in the experiment (day 4) and therefore excluded from the analysis.

Experimental Design

A gradient of 7 CO₂ concentrations (ambient to on average ~1140 µatm) was established in 3 steps over 3 days (day 0 until day 2) by adding differential amounts [between 35 L (M7) and 70 L (M6)] of CO₂-saturated seawater evenly to the water columns of M2–M8 with a custom-made distribution device (Riebesell et al., 2013). M5 was left unperturbed and served as a control but received non-aerated seawater during CO₂ manipulations. CO₂-saturated seawater had to be added at regular intervals during the experiment (days 6, 8, 10, 14, 18, and 25) to counteract CO₂ outgassing at the surface. On day 18, we added NaNO₃, Na₂HPO₄, and Na₂SiO₃ (3.43 ± 0.32, 0.16 ± 0.01, 1.63 ± 0.12 µmol L⁻¹, mean ± SD between



mesocosms) to each mesocosm to simulate an upwelling event of nutrient rich deep-water.

Sampling

Sinking detritus is collected in the terminal end of the sediment trap and removed from there through a hose connected to a vacuum system (Boxhammer et al., 2016). Sediment traps were emptied every second day to avoid resuspension and anoxic conditions at the bottom of the mesocosms.

Water samples from each mesocosm were collected between 9:00 and 11:00 a.m., either every second day (day -2-17 and 25-29) or daily (day 19-25) to obtain higher temporal

resolution right after nutrient fertilization. Sampling was slightly later on day -3 (1:00-2:30 p.m.) since we wanted to have samples directly after filling the mesocosms with seawater. As sampling gear, we used 2.5 m long polypropylene pipes equipped with a pulley system to close the tube at the upper and the lower end. The pipe was left open on both ends and carefully lowered vertically into the water column until the lower end reached a depth of 2.5 m. The upper and the lower end were then closed from the surface with the pulley system, thereby enclosing a vertically integrated water sample. The integrated sample was gently mixed and transferred from the pipes into different sampling bottles. Between 3 and 5

hauls with the pipes were made to sample enough volume for all measurements.

Samples for dissolved inorganic carbon (DIC), total alkalinity (TA), and dissolved inorganic nutrient concentrations [$\text{NO}_3^- + \text{NO}_2^-$, NH_4^+ , PO_4^{3-} , Si(OH)_4] were transferred directly from the sampling tubes into air-tight 1 L polycarbonate (carbonate chemistry) and 0.25 L polyethylene (PE) bottles (nutrients), respectively. DIC samples were carefully transferred in the 1 L bottles allowing considerable overflow before closing them with negligible headspace (i.e., <1 mL). Both carbonate chemistry and nutrient samples were transported in a cooling box to the land-based laboratories of the Plataforma Oceánica de Canarias (PLOCAN) which is located next to Taliarte harbor and hosted our study (Figure 1). DIC and TA samples were pumped from the 1 L bottles through a syringe filter (0.2 μm , Whatman) into air-tight 50 mL glass bottles (DIC) and 100 mL PE bottles (TA, nutrients), respectively. We allowed considerable overflow before closing the DIC glass bottles to minimize gas exchange. Filtered DIC, TA, and nutrient samples were stored at 4°C until analysis on the same day.

The seawater used to measure chlorophyll *a* (chl_a) and biogenic silica (BSi) concentrations, as well as diatom cell abundance, was carefully transferred from the sampling tubes into 10 L PE carboys and transported into a climate chamber at PLOCAN set to 15°C. Chl_a and BSi samples were tapped from the carboys (0.5–0.2 L depending on concentration), filtered ($\Delta\text{pressure} = 200$ mbar) on glass fiber filters (chl_a, GF/F nominal pore size = 0.7 μm) or cellulose acetate filters (BSi, pore size = 0.65 μm), and stored at –20°C until analysis. Microscopy samples were transferred from the carboys in 200 mL brown glass bottles, fixed with acidic Lugol solution (1% final concentration), and stored for maximally 5 months at room temperature until analysis.

Mesozooplankton (MesoZP) samples were collected every 4 days between 11 a.m. and 1 p.m. with vertical net hauls from 2.5 m to the surface. Sampling was carried out with a 0.6 m long Apstein net (55 μm mesh size), which had a 0.09 m diameter cone-shaped opening. Two consecutive net hauls per mesocosm during every sampling resulted in a sample volume of 32 L for each mesocosm.

Temperature (T) and salinity (S) were measured on every sampling day around noon time with a hand-held self-logging CTD probe (CTD60M, Sea and Sun Technologies). Average T and S were calculated by averaging the vertical profile from the surface (0.3 m) to the bottom of the sediment traps (~3.5 m).

Analytical Procedures

$\text{NO}_3^- + \text{NO}_2^-$ (NO_x^-), PO_4^{3-} (P), and Si(OH)_4 (Si) concentrations were measured photometrically within 10 h after sampling (Hansen and Koroleff, 1999). NH_4^+ concentrations were measured fluorometrically in the same timeframe (Holmes et al., 1999). Precision of nutrient measurements was generally well below $\pm 10\%$ as determined with triplicate measurements of each sample. DIC concentrations were measured within 10 h after sampling with an Autonomous Infra-Red Inorganic Carbon Analyser (AIRICA) system (Marianda, Kiel, Germany). Each sample was measured three times and the precision was in most

cases better than $\pm 3 \mu\text{mol kg}^{-1}$. TA was determined in an open cell titration within 24 h after sampling (Dickson et al., 2003). Each sample was measured twice with a precision that was in most cases better than $\pm 4 \mu\text{mol kg}^{-1}$. Both DIC and TA measurements were accuracy-controlled by measurements of certified reference materials (Dickson et al., 2007). $p\text{CO}_2$ partial pressure was calculated from measured (water-column averaged) temperature and salinity, as well as concentrations of DIC, TA, PO_4^{3-} and Si(OH)_4 using Seacarb (Lavigne et al., 2011). We used the recommended default setting and the carbonate dissociation constants (K_1 and K_2) determined by Lueker et al. (2000). Chl_a was extracted 1–2 days after sampling in acetone (90%) in plastic vials, by homogenization of the filters using glass beads and a cell mill (5 min). After centrifugation (10 min, 800 g, 4°C), the supernatant was analyzed on a fluorometer (TURNER 10-AU) following Welschmeyer (1994). The fluorometer was calibrated with spinach chl_a extract as described by Strickland and Parsons (1972). BSi concentrations were determined by leaching the samples with 0.1 M NaOH for 135 min at 85°C. The leaching process was terminated with 0.05 M H₂SO₄ and dissolved silicate was measured by spectrophotometry following Hansen and Koroleff (1999).

Diatom samples were transferred from the brown glass sampling bottles into 25–100 mL Utermöhl chambers. After at least 24 h of sedimentation, cells were counted with an inverted light microscope (Zeiss Axiovert 100). Cells were classified to the lowest identifiable taxonomical level. Diatom cell volumes were estimated following Olenina et al. (2006). We tried to measure the relevant shape dimensions needed for the geometrical formulas but in cases where this was not possible we used species dimensions provided by Olenina et al. (2006) (see Table 1). Carbon biomasses of individual species ($\mu\text{g C L}^{-1}$) were calculated with the volume to carbon transfer functions provided by Menden-Deuer and Lessard (2000). Diatom diversity was estimated with the Shannon Weaver diversity index (H'):

$$H' = - \sum_i \frac{B_i}{B_{\text{total}}} \cdot \ln \frac{B_i}{B_{\text{total}}} \quad (1)$$

where B_i is the C biomass of diatom species *i* and B_{total} the C biomass of all diatoms. Higher H' is equivalent to a higher diversity.

The average cellular carbon quota (C_q) of the diatom community was calculated as:

$$C_q = \frac{\sum_i C_i N_i}{N_{\text{total}}} \quad (2)$$

where C_i is the carbon content of diatom species *i*, N_i is the abundance of diatom species *i*, and N_{total} is the abundance of all diatoms.

MesoZP was preserved with ethanol (70%) and transferred into a Bogorov counting chamber where it was quantified and classified to the lowest possible taxonomic level using a Leica stereomicroscope (MZ12). Copepodites and adult copepods of each species were counted as separate categories but we pooled them for our analysis. Accordingly, MesoZP abundances shown

in this paper are copepodites + adults for each species. *Nauplii* species were not distinguished and counted as one group.

Data Analyses

To analyze the dataset, we split the experiment into 3 consecutive phases. Phase 0 was the time before the CO₂ manipulation (day –3–day –1). Phase I (day 0–day 17) comprised the oligotrophic conditions that prevailed prior to the nutrient addition on day 18. Phase II (day 19–day 29) comprised the phytoplankton bloom that formed under eutrophic conditions after nutrient fertilization. For the analyses we calculated the phase averages of *p*CO₂ (i.e., the independent variable) and the phase averages

of the various dependent variables (e.g., chl *a* or BSi). Shapiro-Wilk tests revealed non-normal distribution of the datasets so that they were log-transformed. Afterward, we ran regression analyses with the log-transformed data using R¹ as in Schulz et al. (2013) and Paul et al. (2015). CO₂ was considered to influence the abundance of individual diatom species when we detected a significant (*p* < 0.05) correlation between *p*CO₂ and diatom abundance.

Dissimilarities in diatom community composition between CO₂ levels were mapped by means of Principal Coordinate

¹<http://www.r-project.org>

TABLE 1 | List of all diatom species enumerated by means of light microscopy.

Species	Shape	Formula	Dimensions (μm)	Volume (μm ³)	C (pg)	Measured/referenced
<i>Actinocyclus</i> spp.	Sphere	$\pi/6 \cdot d^3$	d = 25	8177	429	Measured
<i>Asterionellopsis glacialis</i>	Cone +half Sphere-40%	$(\pi/12 \cdot d^2 \cdot h) - 40\%$	d = 5; h = 30	118	14	Measured
<i>Bacteriatrum hyalinum</i>	Cylinder	$\pi/4 \cdot d^2 \cdot h$	d = 15; h = 20	3533	217	Measured
<i>Cerataulina</i>	Cylinder	$\pi/4 \cdot d^2 \cdot h$	d = 25; h = 80	39250	1531	Measured
<i>Chaetoceros</i> spp. <10 μm	Oval cylinder	$\pi/4 \cdot d_1 \cdot d_2 \cdot h$	d ₁ = 7; d ₂ = 6; h = 7	229	24	Referenced
<i>Chaetoceros</i> spp. >10 μm	Oval cylinder	$\pi/4 \cdot d_1 \cdot d_2 \cdot h$	d ₁ = 13; d ₂ = 10; h = 20	2041	139	Referenced
<i>Chaetoceros affinis</i>	Oval cylinder	$\pi/4 \cdot d_1 \cdot d_2 \cdot h$	d ₁ = 15; d ₂ = 10; h = 25	2944	187	Referenced
<i>Chaetoceros atlanticus</i>	Oval cylinder	$\pi/4 \cdot d_1 \cdot d_2 \cdot h$	d ₁ = 10; d ₂ = 7; h = 10	550	48	Measured
<i>Chaetoceros curvisetus</i>	Oval cylinder	$\pi/4 \cdot d_1 \cdot d_2 \cdot h$	d ₁ = 15; d ₂ = 8; h = 15	1325	98	Referenced
<i>Chaetoceros decipiens</i>	Oval cylinder	$\pi/4 \cdot d_1 \cdot d_2 \cdot h$	d ₁ = 15; d ₂ = 10; h = 11	1295	96	Referenced
<i>Chaetoceros didymus</i>	Oval cylinder	$\pi/4 \cdot d_1 \cdot d_2 \cdot h$	d ₁ = 20; d ₂ = 10; h = 14	2198	148	Referenced
<i>Chaetoceros lauderi</i>	Oval cylinder	$\pi/4 \cdot d_1 \cdot d_2 \cdot h$	d ₁ = 16; d ₂ = 9; h = 28	3165	199	Referenced
<i>Chaetoceros lorenzianus</i>	Oval cylinder	$\pi/4 \cdot d_1 \cdot d_2 \cdot h$	d ₁ = 12; d ₂ = 9; h = 34	2883	184	Referenced
<i>Corethron</i> spp.	Cylinder	$\pi/4 \cdot d^2 \cdot h$	d = 20; h = 80	25120	1066	Measured
<i>Cylindrotheca</i> spp.	Rotational Ellipsoid	$\pi/6 \cdot d^2 \cdot h$	d = 5; h = 80	1047	81	Measured
<i>Dactyliosolen</i> spp.	Cylinder	$\pi/4 \cdot d^2 \cdot h$	d = 10; h = 55	4318	256	Measured
<i>Eucampia zodiacus</i>	Oval cylinder	$\pi/4 \cdot d_1 \cdot d_2 \cdot h$	d ₁ = 20; d ₂ = 8; h = 10	1256	94	Referenced
<i>Eunotia clevei</i>	Oval cylinder	$\pi/4 \cdot d_1 \cdot d_2 \cdot h$	d ₁ = 10; d ₂ = 5; h = 20	785	64	Measured
<i>Guinardia delicatula</i>	Cylinder	$\pi/4 \cdot d^2 \cdot h$	d = 25; h = 60	29438	1212	Measured
<i>Guinardia</i> spp. <20 μm	Cylinder	$\pi/4 \cdot d^2 \cdot h$	d = 20; h = 170	53380	1965	Measured
<i>Guinardia</i> spp. >20 μm	Cylinder	$\pi/4 \cdot d^2 \cdot h$	d = 25; h = 150	73593	2549	Measured
<i>Helicotheca</i> spp.	Parallelepiped	$l \cdot w \cdot h$	l = 50; w = 20; h = 5	5000	288	Measured
<i>Hemiaulus hauckii</i>	Oval cylinder	$\pi/4 \cdot d_1 \cdot d_2 \cdot h$	d ₁ = 20; d ₂ = 10; h = 60	9420	481	Measured
<i>Leptocylindrus</i> spp.	Cylinder	$\pi/4 \cdot d^2 \cdot h$	d = 5; h = 28	589	51	Referenced
<i>Leptocylindrus</i> spp. >5 μm	Cylinder	$\pi/4 \cdot d^2 \cdot h$	d = 7; h = 30	1154	88	Measured
<i>Licmophora</i> spp.	Half parallelepiped	$l \cdot w \cdot h/2$	l = 35; w = 15; h = 3	788	64	Measured
<i>Navicula</i> spp.	Parallelepiped	$l \cdot w \cdot h$	l = 25; w = 5; h = 5	375	35	Referenced
<i>Nitzschia</i> spp. <50 μm	Half parallelepiped	$l \cdot w \cdot h/2$	l = 40; w = 3; h = 3	180	19	Referenced
<i>Nitzschia</i> spp. >50 μm	Half parallelepiped	$l \cdot w \cdot h/2$	l = 80; w = 4; h = 4	640	54	Measured
<i>Pleurosigma</i> spp.	Oval cylinder	$\pi/4 \cdot d_1 \cdot d_2 \cdot h$	l = 110; w = 16; h = 9.6	11827	579	Referenced
<i>Pseudo-nitzschia</i> spp. <60 μm	Parallelepiped	$l \cdot w \cdot h$	l = 55; w = 2.5; h = 2.5	309	30	Referenced
<i>Pseudo-nitzschia</i> spp. >60 μm	Parallelepiped	$l \cdot w \cdot h$	l = 110; w = 3; h = 3	792	65	Referenced
<i>Rhizosolenia</i> spp.	Cylinder	$\pi/4 \cdot d^2 \cdot h$	d = 15; h = 250	44156	1685	Measured
<i>Skeletonema costatum</i>	Cylinder	$\pi/4 \cdot d^2 \cdot h$	d = 10; h = 21	1649	117	Referenced
<i>Thalassiosira</i> spp.	Cylinder	$\pi/4 \cdot d^2 \cdot h$	d = 45; h = 22.5	35767	1420	Referenced
<i>Thalassiosira constricta</i>	Cylinder	$\pi/4 \cdot d^2 \cdot h$	d = 15; h = 18	3179	199	Measured
<i>Thalassionema nitzschioides</i>	Parallelepiped	$l \cdot w \cdot h$	l = 45; w = 5; h = 5	1125	86	Referenced

d, diameter; *h*, height; *l*, length; *w*, width. Measured or referenced indicates whether the dimensions to calculate cell volumes were measured or if they were adopted from Olenina et al. (2006).

Analyses (PCoA) using C biomass data ($\mu\text{mol C L}^{-1}$) from the most important diatom genera: *Guinardia*, *Rhizosolenia*, *Cerataulina*, *Thalassiosira*, *Dactyliosolen*, *Chaetoceros*, *Skeletonema*, *Leptocylindrus*, and *Pseudo-nitzschia*. C biomass data from each species were averaged for phase 0, I, and II to yield one separate dataset for each phase. Two-dimensional PCoA plots ($k = 2$) were generated thereafter with Bray-Curtis dissimilarity matrices using the ‘vegan’ package for R (Oksanen et al., 2018).

RESULTS

Physicochemical Conditions

The average temperature was initially $17.73 \pm 0.01^\circ\text{C}$ (day -3 ; mean of all mesocosms \pm SD) and increased only marginally to $18.86 \pm 0.05^\circ\text{C}$ at the end of the study. Temperature developments were almost identical in all mesocosms and closely followed the temperatures in the surrounding water since the heat transfer between the inside and outside of the mesocosms is extremely fast (Bach et al., 2016). The average salinity inside the mesocosms was initially 36.98 ± 0.04 but increased to 38.48 ± 0.08 at the end of the experiment (day 29) due to evaporation (please note that the initial salinity measurement comes from day 1 because the salinity sensor was malfunctioning from day -3 to day 1). Salinity outside the mesocosms was constant around 37 and the salinity increase must be seen as a mesocosm artifact. However, since the salinity increase was almost identical in all mesocosms, it cannot be responsible for the observed CO₂-dependent differences in the plankton communities presented herein.

The injection of different amounts of CO₂-saturated seawater at the beginning of the experiment resulted in the expected $p\text{CO}_2$ gradient, ranging from 375 (ambient) to 1406 μatm on day 3. The relative $p\text{CO}_2$ gradient between the mesocosms was maintained throughout the experiment, although the absolute $p\text{CO}_2$ values varied. A considerable decline of $p\text{CO}_2$ was observed in all mesocosms after the nutrient fertilization due to the net uptake of CO₂ by phytoplankton (Figure 2A).

At the beginning of the study (day -3), nutrient concentrations were 1.46 ± 0.27 , 0.17 ± 0.02 , 1.29 ± 0.2 , $0.47 \pm 0.15 \mu\text{mol L}^{-1}$ for NO_x⁻, P, Si, and NH₄⁺, respectively. These nutrient concentrations were well within the natural range observed in the surface at the nearby European Station for Time Series in the Ocean at the Canary Islands (ESTOC), located in the NE Atlantic subtropical gyre (Cianca et al., 2007). Nutrient concentrations were declining from day -3 onward but at different rates (NO_x⁻ > NH₄⁺ > Si > P; Figure 2). All nutrients were exhausted by the end of phase I and hence before nutrient enrichment on day 18 (Figure 2).

NO_x⁻, P, and Si concentrations were moderately increased on day 18 and averaged at 3.43 ± 0.32 , 0.16 ± 0.01 , and $1.63 \pm 0.12 \mu\text{mol L}^{-1}$ directly after the nutrient enrichment. These N:P:Si ratios roughly correspond to those of deep water (~ 600 m) around the study area (Taucher et al., 2017). The fertilization induced phytoplankton growth and corresponding nutrient drawdown. NO_x⁻ declined fastest reaching values from

before the bloom between days 23–25, and on day 27 in the 619 μatm treatment (Figure 2B). P reached pre-bloom values between days 27 and 29, albeit not in the 1137 μatm treatment (Figure 2C). Si reached pre-bloom values between days 25 and 27 in the three highest CO₂ treatments, whereas Si remained at significantly ($p < 0.05$) higher levels in the two lowest CO₂ mesocosms until the end of the experiment ($> 1 \mu\text{mol L}^{-1}$; Figure 2D). NH₄⁺ was not added during the nutrient enrichment but concentrations showed a higher day to day variability during phase II (Figure 2E).

Bulk Phytoplankton

Chla concentrations were $0.73 \pm 0.07 \mu\text{mol L}^{-1}$ on the first sampling day (day -3) and increased quickly to $2 \pm 0.04 \mu\text{mol L}^{-1}$ on day -1 (Figure 2F), consistent with the decreasing nutrient concentrations (Figures 2B–E). Chla dropped down to the initial values on day 1 and remained quite constant at this level throughout phase I. Chla was slightly, but significantly elevated in the high CO₂ treatments during phase I ($p = 0.043$, Figure 2F). The nutrient enrichment on day 18 led to a rapid chla increase in all mesocosms except for the 619 μatm treatment. Here, the increase was delayed since the chla concentration at the onset of the bloom was considerably lower than in the other mesocosms (check Figure 2F on day 18). CO₂ had no significant influence on chla during phase II.

Biogenic silica concentrations were $0.36 \pm 0.07 \mu\text{mol L}^{-1}$ on the first sampling day (day -3). Concentrations increased thereafter in all mesocosms until peaking at $1.5 \pm 0.1 \mu\text{mol L}^{-1}$ on day 7. BSi declined after the peak to $0.22 \pm 0.11 \mu\text{mol L}^{-1}$ at the end of phase I (Figure 2G). CO₂ had a significant positive influence on the BSi development after the nutrient fertilization ($p = 0.002$). BSi increased to values slightly lower than $2 \mu\text{mol L}^{-1}$ in the three highest CO₂ mesocosms (day 29), while hardly any increase was observed in the two lowest CO₂ mesocosms (day 29; Figure 2G). The BSi development over the course of the study is reflected in the development of dissolved Si (compare Figures 2D,G; please note that the BSi decline at the end of phase I is not leading to increasing concentrations of dissolved Si since the BSi sinks out into the sediment traps and is therefore removed from the water columns).

Diatom Communities

The diatom community was initially diverse (Figure 2H) and dominated by species that are frequently found in the region (Anabalón et al., 2014). The genera with highest C biomass contribution in the mesocosms were: *Guinardia* (Guin), *Rhizosolenia* (Rhiz), *Cerataulina* (Cera), *Thalassiosira* (Thals), *Dactyliosolen* (Dact), *Chaetoceros* (Chae), *Skeletonema* (Skel), *Leptocylindrus* (Lept), and *Pseudo-nitzschia* (Ps-n). These are shown on an individual basis in Figures 3, 4. Subdominant species were pooled and shown as one group (“others,” Figures 3, 4). A full species list with calculated biovolumes and C biomasses is provided in Table 1. The PCoA of phase 0 revealed no treatment-specific dissimilarities between mesocosms before the first CO₂ addition (Figure 5A). The three highest CO₂ treatments were mapped at the extremes of the PCo space. This information is important as it indicates that dissimilarities

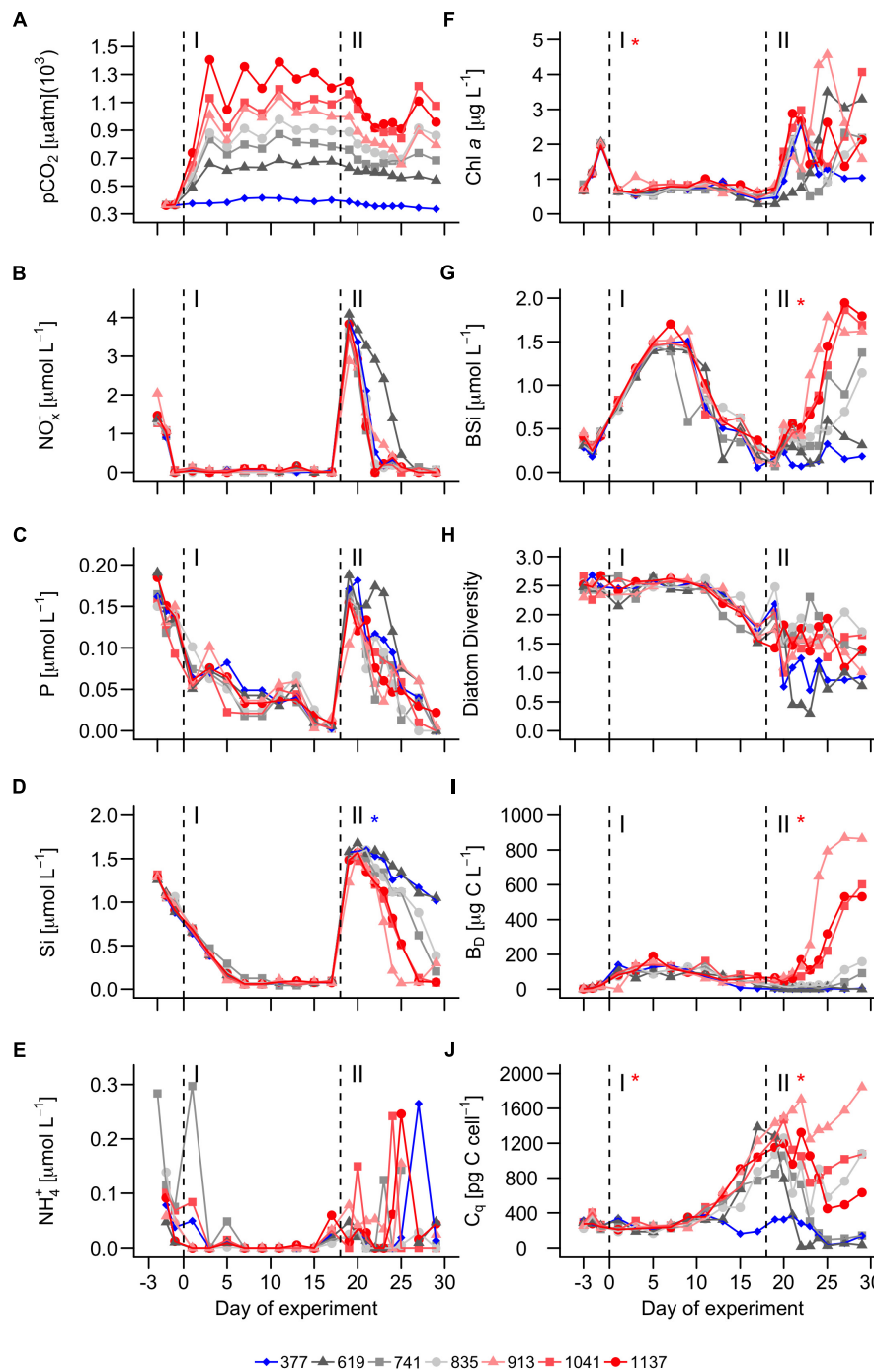


FIGURE 2 | Chemical conditions and bloom formations in the mesocosms. **(A)** pCO₂. **(B)** Nitrate + Nitrite concentrations. **(C)** Phosphate concentration. **(D)** Dissolved silicate concentration. **(E)** Ammonium concentration. **(F)** Chlorophyll *a* concentration. **(G)** Biogenic silica. **(H)** Shannon-Weaver diversity of the diatom community. **(I)** total diatom biomass. **(J)** Cellular C quota averaged over all diatom species (see Eq. 2). Dashed vertical lines separate the three phases of the experiment. Asterisks indicate significantly ($p < 0.05$) positive (red) or negative (blue) CO₂ effects during phases. The legend at the bottom gives mean pCO₂ values (in μatm) of the different treatments.

between treatments later in the experiment are less likely to be predetermined by the initial diatom community structure.

Diatoms started to grow exponentially at the beginning of the study until days 1 to 5, reflected in the BSi build-up and Si

drawdown (**Figures 2D,G**). Abundance and C biomass declined after this initial peak but in some genera (e.g., *Skeletonema*) more than in others (e.g., *Guinardia*; compare **Figures 3A, 4A** with **Figures 3G, 4G**). The decline of some species to almost

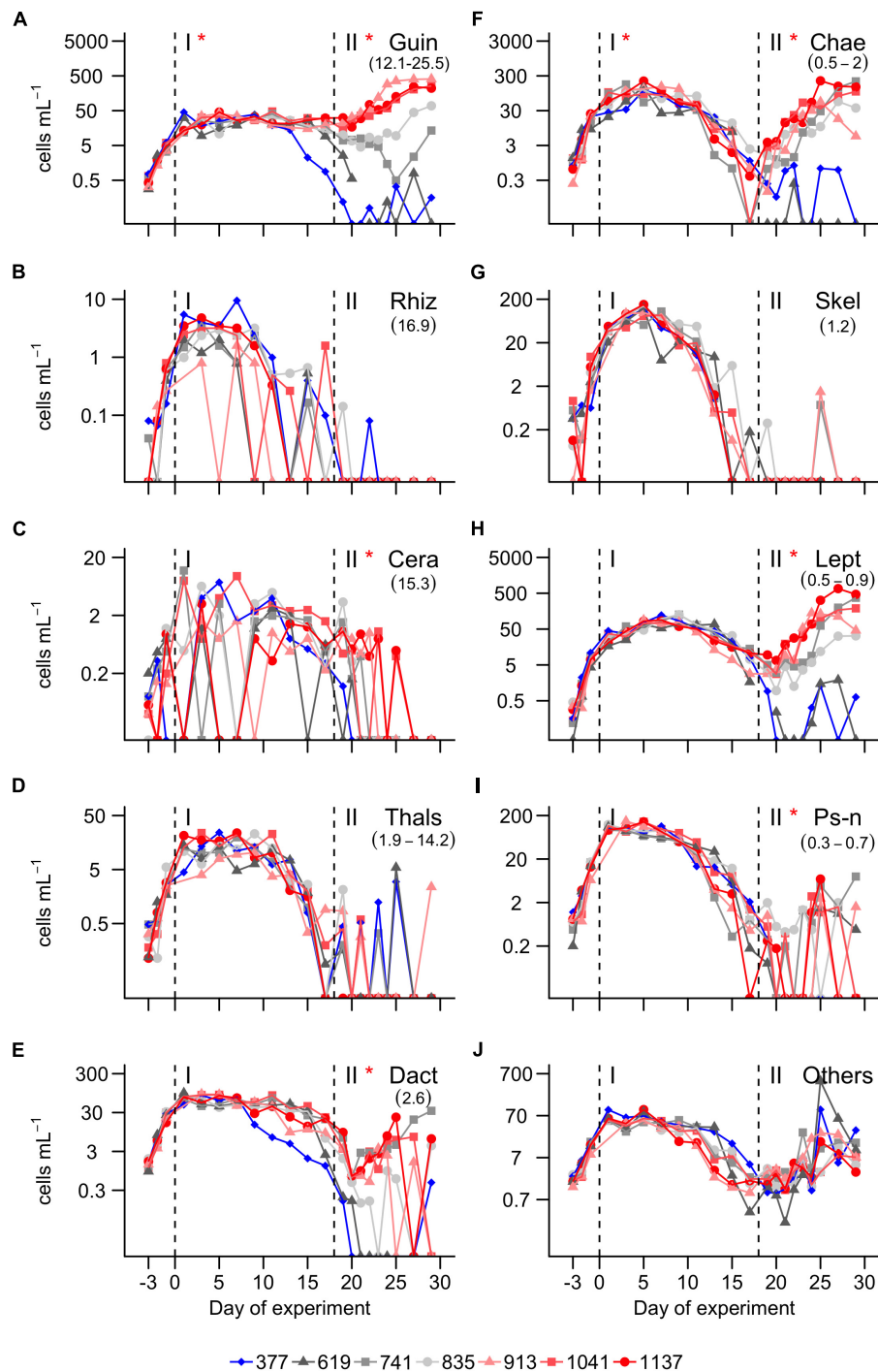


FIGURE 3 | Abundance of the most important diatom genera. **(A)** *Guinardia*. **(B)** *Rhizosolenia*. **(C)** *Cerataulina*. **(D)** *Thalassiosira*. **(E)** *Dactyliosolen*. **(F)** *Chaetoceros*. **(G)** *Skeletonema*. **(H)** *Leptocylindrus*. **(I)** *Pseudo-nitzschia*. **(J)** Sum of all other diatom species. A full species list is provided in **Table 1**. Dashed vertical lines separate the three phases of the experiment. Asterisks indicate significantly ($p < 0.05$) positive (red) or negative (blue) CO₂ effects during phases. The legend at the bottom gives mean $p\text{CO}_2$ values (in μatm) of the different treatments.

undetectable abundances toward the end of phase I led to a decrease of diversity from ~ 2 (days -3 – 13) to ~ 1.2 (days 17 – 29 ; **Figure 2H**). Diatoms developed similarly in all treatments during the more oligotrophic conditions in phase I, but we

detected significant CO₂ effects on abundance and C biomass of *Guinardia* and *Chaetoceros* (**Figures 3A,F** and **Table 2**). C_q (Eq. 2) of the diatom community averaged over phase I was positively correlated with $p\text{CO}_2$ (**Figure 2J**). The PCoA of

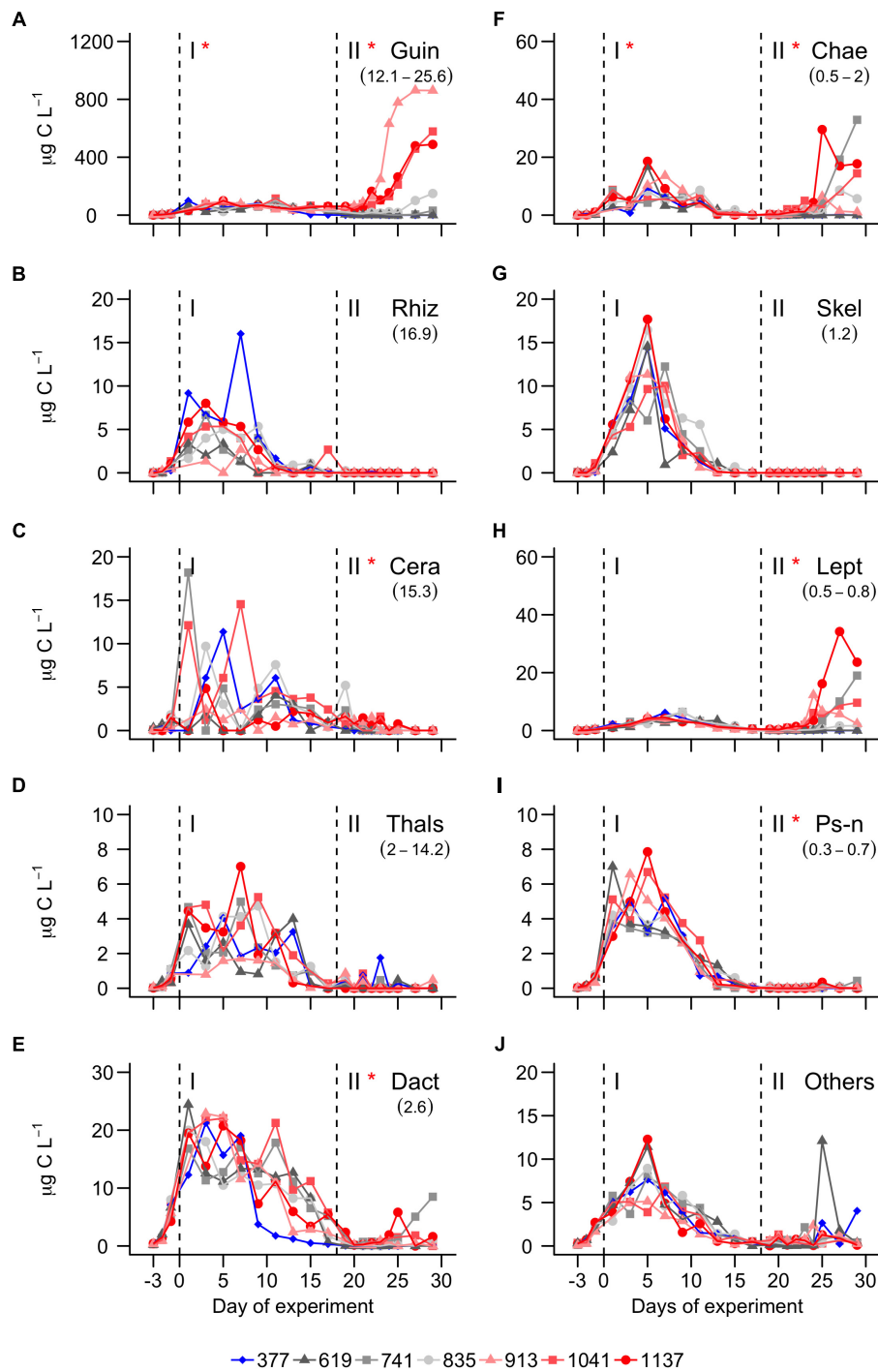


FIGURE 4 | C Biomass of the most important diatom genera. **(A)** *Guinardia*. **(B)** *Rhizosolenia*. **(C)** *Cerataulina*. **(D)** *Thalassiosira*. **(E)** *Dactyliosolen*. **(F)** *Chaetoceros*. **(G)** *Skeletonema*. **(H)** *Leptocylindrus*. **(I)** *Pseudo-nitzschia*. **(J)** Sum of all other diatom species. A full species list is provided in **Table 1**. Dashed vertical lines separate the three phases of the experiment. Asterisks indicate significantly ($p < 0.05$) positive (red) or negative (blue) CO₂ effects during phases. The legend at the bottom gives mean pCO_2 values (in μatm) of the different treatments.

phase I revealed no pronounced CO₂-dependent dissimilarities of the diatom communities, although there is, perhaps, a mild separation between the three highest CO₂ mesocosms and the control along PCo1 (**Figure 5B**).

A pronounced diatom bloom was initiated through the nutrient fertilization at the beginning of phase II. However, the onset of the bloom varied among the different diatom genera. While *Chaetoceros* was responding immediately (day 18), it took

most of the other genera a few days before they started to grow (Figure 3B). Nanoflagellates (0.2–2 μm) were profiting from this delay (Filella et al., 2018) and were largely responsible for the first chl *a* peak on day 22, shortly after nutrient fertilization (Figure 2B). Diatoms became more influential on the bulk chl *a* signal about 1 week after fertilization (compare Figures 2B, 4), although other groups like non-diazotrophic cyanobacteria, dinoflagellates, or nanoflagellates still had a noticeable influence (Filella et al., 2018).

CO₂ had a strong influence on the composition of the diatom assemblage after the nutrient fertilization. Abundance and C biomass of *Cerataulina*, *Chaetoceros*, *Dactyliosolen*, *Guinardia*, *Leptocylindrus*, and *Pseudo-nitzschia* were significantly positively influenced under high CO₂. *Guinardia* was the species with the highest carbon content and profited most strongly from high CO₂ levels (Figures 3D, 4D). C_q of the diatom community was positively correlated with pCO₂ during phase I and II (Figure 2I, phase I, *p* = 0.022; phase II *p* = 0.009). The PCoA for phase II revealed CO₂-dependent dissimilarities of the diatom community where the control and the 619 μatm treatment, the 741 and the 835 μatm treatments, and the three highest CO₂

treatments were mapped in three different regions of the PCo space (Figure 5C).

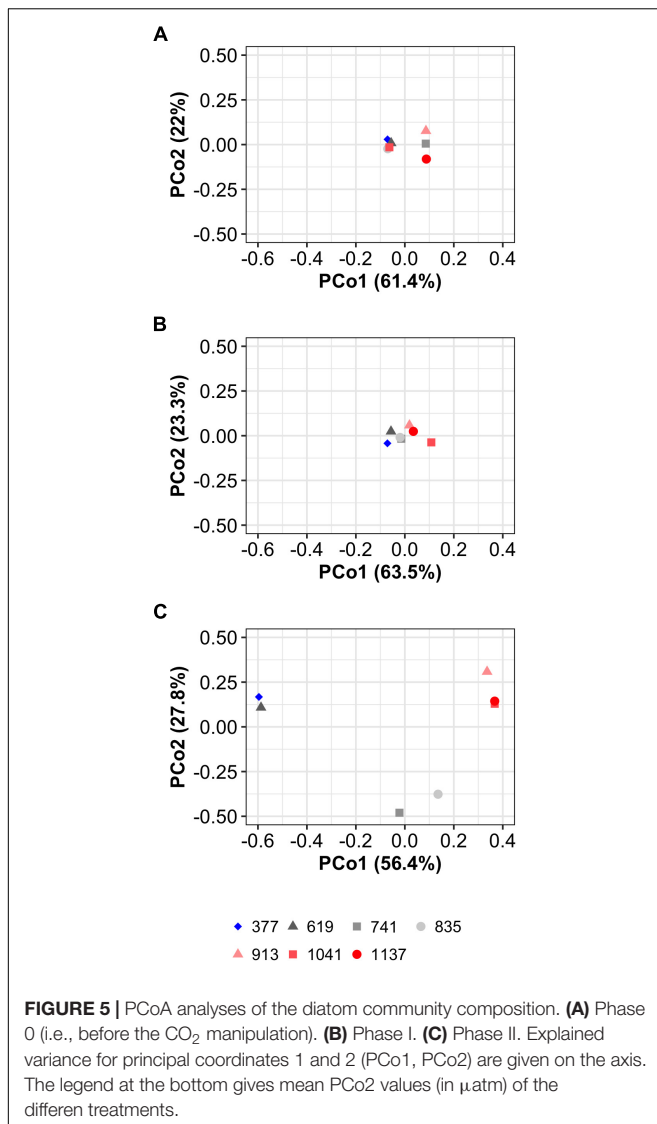
Mesozooplankton

The MesoZP communities were numerically dominated by copepods (Figure 6). Individuals of the different species were generally small with even the adults hardly ever being larger than 500 μm. The two genera *Clausocalanus* and *Paracalanus* were not distinguishable while counting the sample and were therefore merged into one taxonomic unit, termed *CP-calanus* in the following (please note that both genera were present in the mesocosms as was determined with meta-barcoding). The most abundant copepod genera during phase I were *CP-calanus*, *Oithona*, *Oncaea*, and *Temora* (Figures 6A,C,E,F). *CP-calanus* and *Temora* reached particularly high abundances during phase II but only in the lower CO₂ mesocosms (Figures 6A,E). Copepod nauplii reached abundance peaks on days 13 and 30, although there was a large spread among mesocosms especially during the second peak (Figure 6H). Other MesoZP taxa that occurred in high abundances comprised *Oikopleura dioica* (appendicularia) and foraminifera (most likely *Globigerinidae*

TABLE 2 | Statistics; Regression analyses were performed for time-averaged means for the two experimental phases.

Dependent variable	Phase	<i>p</i> -value	<i>R</i> ²	F statistic	Phase	<i>p</i> -value	<i>R</i> ²	F statistic
NO _x ⁻	I	0.728	0.03	0.135	II	0.307	0.21	1.292
PO ₄ ³⁻	I	0.601	0.06	0.313	II	0.174	0.34	2.514
Si(OH) ₄	I	0.621	0.05	0.276	II	0.024	0.67	10.17
NH ₄	I	0.931	0.01	0.008	II	0.733	0.03	0.13
Chlorophyll <i>a</i>	I	0.043	0.59	7.268	II	0.081	0.49	4.776
BSi	I	0.215	0.21	1.372	II	0.001	0.79	19.1
H'	I	0.932	0.01	0.008	II	0.151	0.36	2.866
B _D	I	0.189	0.32	2.312	II	0.006	0.81	20.96
C _q	I	0.022	0.67	10.62	II	0.009	0.77	16.69
<i>Guinardia</i>	I	0.041	0.60	7.492	II	0.002	0.88	35.2
<i>Rhizosolenia</i>	I	0.451	0.12	0.666	II	0.464	0.11	0.627
<i>Cerataulina</i>	I	0.833	0.01	0.05	II	0.023	0.68	10.46
<i>Thalassiosira</i>	I	0.707	0.03	0.157	II	0.13	0.39	3.283
<i>Dactyliosolen</i>	I	0.161	0.35	2.71	II	0.05	0.57	5.534
<i>Chaetoceros</i>	I	0.006	0.81	21.02	II	0.015	0.81	17.05
<i>Skeletonema</i>	I	0.454	0.12	0.656	II	0.847	0.01	0.041
<i>Leptocylindrus</i>	I	0.218	0.28	1.983	II	0.015	0.73	13.32
<i>Pseudo-nitzschia</i>	I	0.298	0.21	1.346	II	0.044	0.6	7.162
Others	I	0.613	0.11	0.469	II	0.201	0.31	2.162
<i>Clauso-/Paracalanus</i>	I	0.79	0.02	0.079	II	0.022	0.68	10.73
<i>Nannocalanus</i>	I	0.953	0.01	0.004	II	0.212	0.29	2.05
<i>Oncaea</i>	I	0.929	0.01	0.009	II	0.699	0.03	0.167
<i>Oikopleura</i>	I	0.438	0.12	0.71	II	–	–	–
<i>Temora</i>	I	0.295	0.21	1.364	II	0.026	0.66	9.883
<i>Oithona</i>	I	0.641	0.05	0.246	II	0.021	0.69	10.91
Foraminifera	I	0.121	0.41	3.487	II	0.403	0.14	0.833
Copepoda nauplii	I	0.729	0.03	0.134	II	0.934	0.01	0.008

Results were considered to be statistically significant if the correlation between pCO₂ (independent variable) and the dependent variable revealed a significant trend (*p* < 0.05). Please note that results were identical for diatom abundances and C biomasses so that the statistical outcomes apply for both. The bold values indicate statistical significance.



species). *O. dioica* was initially not detected but occurred suddenly in some mesocosms during phase I (Figure 6D). It disappeared equally quickly after the bloom and remained detectable only in the 619 and 913 μ atm treatments (Figure 6D). Foraminifera were detected in low abundances since the first sampling and they thrived in all mesocosms until day 21–25 (Figure 6G).

CO₂ effects on MesoZP were detected only in 3 species and only in phase II. CO₂ had a strong positive influence on the abundance of *CP-calanus* and *Temora* (Figures 6A,E). *Oithona* was negatively affected by CO₂ but the effect was not as pronounced as in the two other genera (Figure 6F).

DISCUSSION

Physiological studies have shown that growth and the metabolism of diatoms can be affected by increasing seawater CO₂

concentrations (Gao and Campbell, 2014). A recent meta-analysis of OA laboratory experiments with diatoms revealed an increase of growth rates under high CO₂, although the response varies widely among different diatom species (Dutkiewicz et al., 2015). This inter-specific variability is an important feature as it suggests that high CO₂ conditions will affect diatom species differentially and therefore, alter the composition of diatom assemblages (Tortell et al., 2008; Hoppe et al., 2013; Endo et al., 2016). Indeed, our experiment revealed a positive effect on the bulk diatom biomass (C_q) that coincided with shifts in the assemblage structure after the nutrient addition.

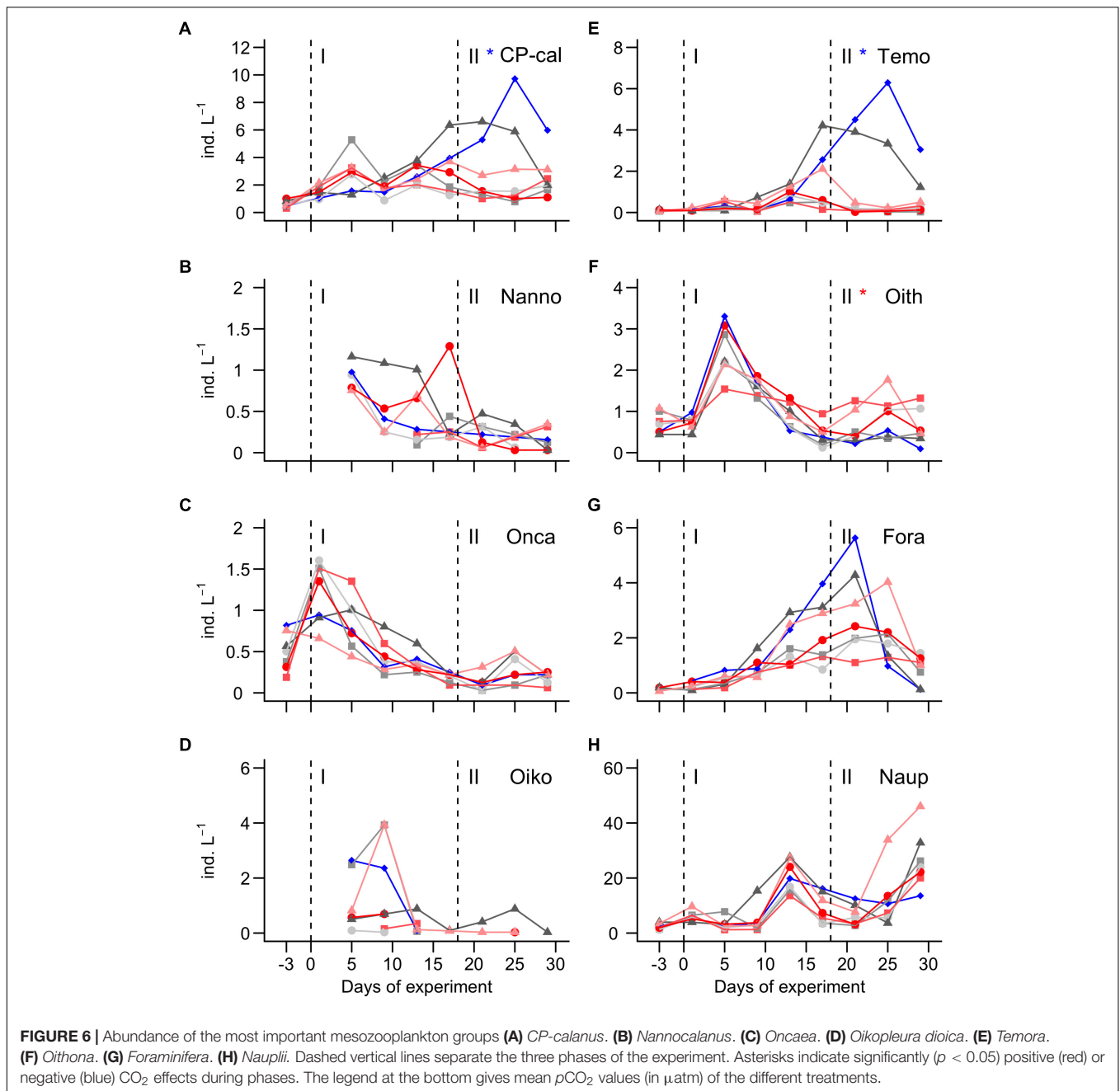
The exact mechanisms which control diatom responses to high CO₂ are difficult to uncover in mesocosm experiments because the complexity of the food web allows a myriad of explanations (Bach et al., 2017). Therefore, our goal in the discussion is not to mention every imaginable mechanism but to highlight particularly plausible ones while acknowledging that none of them can be proven and none are necessarily exclusive. In fact, several mechanisms could coincide and ultimately explain the observed responses together. After discussing potential mechanisms underlying the observed CO₂ responses (section “Potential Mechanisms Explaining Observed CO₂ Effects on the Diatoms”), we consider our findings in a wider perspective and discuss their value to assess diatom responses to OA in the subtropical NE Atlantic (section “What Can These Results Tell Us About OA Impacts on Diatoms in the Subtropical NE Atlantic?”).

Potential Mechanisms Explaining Observed CO₂ Effects on the Diatoms

CO₂ Fertilization of Photosynthesis

When phytoplankton profits from high CO₂ then this is usually explained with a CO₂ fertilization effect on inorganic carbon acquisition. The idea is that increasing seawater p CO₂ facilitates the diffusive uptake of CO₂, thereby reducing the energy demand for active carbon acquisition (Giordano et al., 2005; Reinfelder, 2011). The energy that is saved by reducing the operation of this so-called “carbon concentrating mechanism (CCM)” can be diverted into the acquisition of other resources, ultimately leading to faster growth. Physiological studies with diatoms generally support this concept, although variability exists between species (Rost et al., 2003; Hopkinson et al., 2011; Trimborn et al., 2013; Gao and Campbell, 2014).

The CCM related explanation may also apply to our results. Elevated p CO₂ may have stimulated resource acquisition in some of the diatom species present in the mesocosms, thereby leading to CO₂-dependent restructuring of the assemblage. Recently, Wu et al. (2014) performed laboratory CO₂ experiments with four different *Thalassiosira* species and *Coscinodiscus wailesii*, and found that the CO₂ fertilization effect on growth rates scales positively with cell volume. Although their concept is derived mainly from one genus, it is physiologically well substantiated and based on the positive correlation between cell size and diffusion gradients, which predicts that high CO₂ is particularly beneficial for carbon acquisition in larger species (Pasciak and Gavis, 1974; Wolf-Gladrow and Riebesell, 1997; Flynn et al., 2012; Shen and Hopkinson, 2015). Applying the cell volume



dependency determined by Wu et al. (2014) to our dataset partially confirms their concept. As predicted, we observed by far the strongest CO₂ stimulation in *Guinardia*, the largest genus present in the experiment. Apart from *Guinardia*, however, CO₂ effects did not seem to scale with diatom biovolumes. There were small genera (e.g., *Chaetoceros*) that showed clearer CO₂ responses than larger ones (e.g., *Cerataulina*) (Figures 3C,F). Hence, while the Wu et al. (2014) concept provides a great starting point to interpret results observed in field experiments, it still needs to be expanded to account for the ecological complexities occurring outside the laboratory environment and genotype-specific variability. The application of molecular tools

in community studies may help to make significant progress on that matter (Endo et al., 2016).

CO₂ Effect Through Grazer Interactions

Copepods were the most abundant MesoZP group present in the mesocosms and probably had a top-down impact on the diatom community. Three of the five dominant copepod genera were significantly influenced by high CO₂ during phase II. *Oithona* abundance ranged between 100 and 1800 individuals L⁻¹ and was positively affected (Figure 6F). In contrast, *CP-calanus* and *Temora* abundances ranged between 800 to 9700 and 30 to 6900 individuals L⁻¹, respectively, and were both negatively affected

by high CO₂ (Figures 6A,E). The higher abundances of *CP-calanus* and *Temora*, as well as the larger CO₂ effect size relative to *Oithona*, suggests that any CO₂-related top-down control was primarily mediated through these two species. Indeed, abundances of several diatom species and bulk diatom biomass were significantly reduced under high CO₂ during phase II and particularly low in the control and the lowest CO₂ treatment (619 μatm), where considerably more *CP-calanus* and *Temora* were present (compare Figures 2I, 6A,E). This anti-correlated pattern points toward a causal relationship between diatom and *CP-calanus*/*Temora* abundances that were altered through CO₂ concentrations. The key question is: Through which mechanisms could CO₂ affect the interaction between copepods and diatoms?

The most straight-forward explanation would be a negative CO₂ effect on the physiological performance of *CP-calanus* and *Temora*. High CO₂/low pH conditions may have reduced growth and grazing of these two copepod genera, thereby reducing their abundances and ultimately grazing pressure on diatoms. To the best of our knowledge, there is no published study to date in which direct CO₂ effects on *CP-calanus* were investigated under controlled laboratory conditions. Such experiments exist for *Temora longicornis* but it is unclear whether the *Temora* species in our experiments would show the same insensitivity to high CO₂ as the individuals from the English Channel investigated by McConville et al. (2013). Recent OA experiments with *Calanus glacialis* revealed population-specific CO₂ responses with more robust populations found in naturally CO₂-rich habitats (Thor et al., 2018). These findings suggest that local carbonate chemistry conditions may be a better predictor to assess CO₂ sensitivities of copepods than their taxonomic affiliation (Thor et al., 2018; Zhang et al., 2018). They also suggest that laboratory-based results can only reliably be used to interpret responses observed in experiments with natural assemblages when both experiments were done with individuals from the same population. Thus, with the available data it is not possible to assess the likelihood for such a direct negative CO₂ effect on the metabolism of *CP-calanus* and *Temora*.

Altered interactions between *CP-calanus*/*Temora* and diatoms could also have been provoked through CO₂-induced changes in the nutritional quality of the diatoms. If high CO₂ triggers a physiological response in diatoms, that cause them to be less nutritious, copepod growth would be reduced ultimately leading to lower grazing pressure and higher diatom abundances. A potential explanation for this hypothesis comes from experiments by Rossoll et al. (2012), who found that the diatom *Thalassiosira pseudonana* contained less fatty acids under high CO₂ and the composition of the produced fatty acids had a lower nutritional value. As a consequence, the copepod *Acartia tonsa* fed with these *T. pseudonana* cells grew slower and produced less eggs (Rossoll et al., 2012). Furthermore, carbonate chemistry effects on silicification may have altered the strength of the frustule and therefore the palatability of diatoms (Hamm et al., 2003; Wilken et al., 2011; Friedrichs et al., 2013; Liu et al., 2016). Low seawater pH is considered to be beneficial for the silicification process since opal precipitation does occur in a low pH (pH ~5) compartment of the diatom cell (Vrieling et al., 1999; Martin-Jézéquel et al., 2000). Indeed, Hervé et al. (2012) found

increasing Si incorporation and cellular BSi quota in *T. weissflogii* with decreasing pH from 8 to 7.2. However, other experiments with *T. weissflogii* only found increased Si uptake rates (Milligan et al., 2004) but decreasing BSi quota (Milligan et al., 2004) or BSi/C (Mejía et al., 2013). Thus, with the currently available (and partially controversial) information, it is not possible to assess the relevance of carbonate chemistry dependent silicification changes on grazing but it would be worthwhile to further investigate this important feedback in future studies (Milligan et al., 2004; Mejía et al., 2013; Gao and Campbell, 2014).

What Can These Results Tell Us About OA Impacts on Diatoms in the Subtropical NE Atlantic?

The potential of OA impacts on diatom communities will depend on the degree of future CO₂ increase. In the present experiment, diatom composition was noticeably affected at pCO₂ levels >619 μatm, during the bloom in phase II (Figure 5C). This should not be regarded as a general threshold for diatom OA sensitivity as it is likely to vary regionally, depending on the prevailing diatom community and regional carbonate chemistry conditions. More productive regions near coasts or estuaries have typically larger natural variations in carbonate chemistry (Hofmann et al., 2011; Wallace et al., 2014) and should harbor generalist species, which are less responsive to increased CO₂. Conversely, CO₂ enrichment studies in more stable oceanic environments should be more likely to induce a response (Duarte et al., 2013). Carbonate chemistry conditions at the coast of Gran Canaria are rather stable with comparatively little seasonal fluctuations (González-Dávila et al., 2010), which may explain why quite pronounced changes in the diatom community composition were observed already above 619 μatm.

The experiment discussed in the present paper took place in spring 2016 but we did a similar OA experiment at the coast of Gran Canaria with larger mesocosms already in autumn 2014 (Taucher et al., 2017). In this earlier experiment we also observed profound shifts in the diatom community composition, although the CO₂ threshold above which changes occurred could not be determined (Taucher et al., 2018). The diatom genera *Guinardia* and *Leptocylindrus* were important in both the 2016 and the 2014 study and the comparison of their responses to high CO₂ is valuable because it allows us to assess the “reproducibility” of our findings. *Guinardia* benefitted profoundly from high CO₂ in both experiments which raises confidence that the *Guinardia* species enclosed in the mesocosms (*G. striata* in 2014; *G. delicatula*, *Guinardia* spp. in 2016) could become more competitive in an acidified NE Atlantic. *Leptocylindrus*, however, responded oppositely which could be due to different *Leptocylindrus* genotypes being enclosed in the mesocosms (*L. delicatulum* in 2014; *Leptocylindrus* spp. in 2016). Alternatively, different food web structures could have indirectly caused the opposite responses, for example by altering resource competition or grazing pressure. Such food web related differences could have either developed in the course of the study or were already established at the beginning when the communities were enclosed inside the mesocosms

(Moreno de Castro et al., 2017). In this context it is also important remember that the mesocosm bags were filled with pumps in 2016 (section “Mesocosm Design, Deployment, and Maintenance”) while they were lowered into the water column in 2014 (Taucher et al., 2017). The different filling procedures may have amplified differences in the initial community structure.

The *Guinardia* species enclosed in the mesocosms was a comparatively large diatom and its positive response to high CO₂ drove the significant increase of the average cellular carbon quota (C_q) of the diatom community (Figure 2J). Such a CO₂-induced shift toward larger diatoms was also observed in several earlier OA experiments with natural communities (Tortell et al., 2008; Feng et al., 2009, 2010; Eggers et al., 2014; Bach et al., 2017; Taucher et al., 2018) while the opposite response (i.e., a CO₂-induced shift toward smaller diatoms) was reported only once (Davidson et al., 2016). This suggests that OA will generally favor large diatom species, which is in accordance with the physiological theory described at the beginning of section “Potential Mechanisms Explaining Observed CO₂ Effects on the Diatoms”.

CONCLUSION

In this study we enclosed a natural plankton community from the subtropical NE Atlantic in *in situ* mesocosms to assess their response to simulated future ocean acidification. Our findings suggest that the bulk diatom community in the subtropical NE Atlantic could benefit from high CO₂ conditions projected for the end of this century under nutrient supply (e.g., via seasonal or eddy-induced upwelling). However, the positive CO₂ response of the bulk diatom biomass coincided with pronounced shifts in the diatom species composition because not all diatoms benefitted equally from high CO₂. The largest diatom genus in the mesocosms (*Guinardia*) was particularly CO₂ responsive and its pronounced dominance under high CO₂ caused a significant increase in the average size of the diatom community. The particularly strong CO₂ effect on a large diatom is in accordance with physiological theory and has been observed in earlier studies, which adds confidence to this finding. Nevertheless, the discussed example of the response of *Leptocylindrus* to high CO₂ revealed that many uncertainties are yet to be resolved

REFERENCES

- Anabalón, V., Aristegui, J., Morales, C. E., Andrade, I., Benavides, M., Correa-Ramírez, M. A., et al. (2014). The structure of planktonic communities under variable coastal upwelling conditions off Cape Ghir (31°N) in the Canary Current System (NW Africa). *Prog. Oceanogr.* 120, 320–339. doi: 10.1016/j.pcean.2013.10.015
- Aristegui, J., Barton, E. D., Tett, P., Montero, M. F., García-Muñoz, M., Basterretxea, G., et al. (2004). Variability in plankton community structure, metabolism, and vertical carbon fluxes along an upwelling filament (Cape Juby, NW Africa). *Prog. Oceanogr.* 62, 95–113. doi: 10.1016/j.pcean.2004.07.004
- Armbrust, E. V. (2009). The life of diatoms in the world's oceans. *Nature* 459, 185–192. doi: 10.1038/nature08057
- Bach, L. T., Alvarez-Fernandez, S., Hornick, T., Stuhr, A., and Riebesell, U. (2017). Simulated ocean acidification reveals winners and losers in coastal phytoplankton. *PLoS One* 12:e0188198. doi: 10.1371/journal.pone.0188198

before winners and losers within the diatom community can be determined with high confidence.

DATA AVAILABILITY

The datasets generated for this study are available on request to the corresponding author.

AUTHOR CONTRIBUTIONS

LB, JT, UR, and JA designed the experiments. All authors conducted the experiments. LB, NH-H, JT, CaS, and CIS measured the data. LB and NH-H analyzed the data. NH-H performed the statistical analysis and plotted the data. LB drafted the manuscript. LB, NH-H, JT, CaS, UR, and JA revised the manuscript.

FUNDING

This study was financially supported by Cluster of Excellence “The Future Ocean” at the University of Kiel. JA was supported by a Helmholtz International Fellow Award, 2015 (Helmholtz Association, Germany). NH-H and JA benefited also from the FLUXES project (CTM2015-69392-C3-1-R) funded by the Spanish government (Plan Nacional I+D).

ACKNOWLEDGMENTS

We thank Shaomin Chen, Syrmalena Kotronaki, Peter Fritzsche, Andrea Ludwig, Jana Meyer, Alice Nauendorf, and Lena Soumpasis for measuring carbonate chemistry, nutrient, and BSi samples, Andrea Ludwig for logistical support and CTD operations, Michael Krudewig, Michael Sswat, Peter Kohnert, Mario Deckelnick, and Jan Czerny for construction of the mesocosm infrastructure. Furthermore, we also thank the Oceanic Platform of the Canary Islands (PLOCAN) and its staff for the use of their facilities, and for their help with the logistics and organization of this experiment.

- Bach, L. T., Taucher, J., Boxhammer, T., Ludwig, A., Achterberg, E. P., Algueró-Muñoz, M., et al. (2016). Influence of ocean acidification on a natural winter-to-summer plankton succession: first insights from a long-term mesocosm study draw attention to periods of low nutrient concentrations. *PLoS One* 11:e0159068. doi: 10.1371/journal.pone.0159068
- Barton, E. D., Aristegui, J., Tett, P., Canton, M., García-Braun, J., Hernández-León, S., et al. (1998). The transition zone of the Canary Current upwelling region. *Prog. Oceanogr.* 41, 455–504. doi: 10.1016/S0079-6611(98)00023-8
- Boxhammer, T., Bach, L. T., Czerny, J., and Riebesell, U. (2016). Technical note: sampling and processing of mesocosm sediment trap material for quantitative biogeochemical analysis. *Biogeosciences* 13, 2849–2858. doi: 10.5194/bg-13-2849-2016
- Boyd, P., and Newton, P. (1995). Evidence of the potential influence of planktonic community structure on the interannual variability of particulate organic carbon flux. *Deep Sea Res. Part I Oceanogr. Res. Pap.* 42, 619–639. doi: 10.1016/0967-0637(95)00017-Z

- Brzezinski, M. A., and Nelson, D. M. (1996). Chronic substrate limitation of silicic acid uptake rates in the western Sargasso Sea. *Deep Sea Res. Part II Top. Stud. Oceanogr.* 43, 437–453. doi: 10.1016/0967-0645(95)00099-2
- Cianca, A., Helmke, P., Mouriño, B., Rueda, M. J., Llinás, O., and Neuer, S. (2007). Decadal analysis of hydrography and in situ nutrient budgets in the western and eastern North Atlantic subtropical gyre. *J. Geophys. Res. Ocean.* 112:C07025. doi: 10.1029/2006JC003788
- Davidson, A., McKinlay, J., Westwood, K., Thomson, P., van den Eenden, R., de Salas, M., et al. (2016). Enhanced CO₂ concentrations change the structure of Antarctic marine microbial communities. *Mar. Ecol. Prog. Ser.* 552, 93–113. doi: 10.3354/meps11742
- Dickson, A. G., Afghan, J. D., and Anderson, G. C. (2003). Reference materials for oceanic CO₂ analysis: a method for the certification of total alkalinity. *Mar. Chem.* 80, 185–197. doi: 10.1016/S0304-4203(02)00133-0
- Dickson, A. G., Sabine, C. L., and Christian, J. R. (2007). *Guide to Best Practices for Ocean CO₂ Measurements*. Sidney: North Pacific Marine Science Organization.
- Duarte, C. M., Hendriks, I. E., Moore, T. S., Olsen, Y. S., Steckbauer, A., Ramajo, L., et al. (2013). Is ocean acidification an open-ocean syndrome? understanding anthropogenic impacts on seawater pH. *Estuaries and Coasts* 36, 221–236. doi: 10.1007/s12237-013-9594-3
- Dutkiewicz, S., Morris, J. J., Follows, M. J., Scott, J., Levitan, O., Dyhrman, S. T., et al. (2015). Impact of ocean acidification on the structure of future phytoplankton communities. *Nat. Clim. Chang.* 5, 1002–1006. doi: 10.1038/nclimate2722
- Eggers, S. L., Lewandowska, A. M., Barcelos E Ramos, J., Blanco-Ameijeiras, S., Gallo, F., and Matthiessen, B. (2014). Community composition has greater impact on the functioning of marine phytoplankton communities than ocean acidification. *Glob. Chang. Biol.* 20, 713–723. doi: 10.1111/gcb.12421
- Endo, H., Sugie, K., Yoshimura, T., and Suzuki, K. (2016). Response of Spring Diatoms to CO₂ Availability in the Western North Pacific as Determined by Next-Generation Sequencing. *PLoS One* 11:e0154291. doi: 10.1371/journal.pone.0154291
- Feng, Y., Hare, C. E., Leblanc, K., Rose, J. M., Zhang, Y., DiTullio, G. R., et al. (2009). Effects of increased pCO₂ and temperature on the north atlantic spring bloom. I. The phytoplankton community and biogeochemical response. *Mar. Ecol. Prog. Ser.* 388, 13–25. doi: 10.3354/meps08133
- Feng, Y., Hare, C. E., Rose, J. M., Handy, S. M., DiTullio, G. R., Lee, P. A., et al. (2010). Interactive effects of iron, irradiance and CO₂ on Ross Sea phytoplankton. *Deep. Res. Part I Oceanogr. Res. Pap.* 57, 368–383. doi: 10.1016/j.dsr.2009.10.013
- Field, C. B., Behrenfeld, M. J., Randerson, J. T., and Falkowski, P. G. (1998). Primary Production of the Biosphere: Integrating Terrestrial and Oceanic Components. *Science* 281, 237–240. doi: 10.1126/science.281.5374.237
- Filella, A., Baños, I., Montero, M. F., Hernández-Hernández, N., Rodríguez-Santos, A., Ludwig, A., et al. (2018). Plankton Community Respiration and ETS Activity Under Variable CO₂ and Nutrient Fertilization During a Mesocosm Study in the Subtropical North Atlantic. *Front. Mar. Sci.* 5:310. doi: 10.3389/fmars.2018.00310
- Flynn, K. J., Blackford, J. C., Baird, M. E., Raven, J. A., Clark, D. R., Beardall, J., et al. (2012). Changes in pH at the exterior surface of plankton with ocean acidification. *Nat. Clim. Chang.* 2, 510–513. doi: 10.1038/nclimate1489
- Friedrichs, L., Hörnig, M., Schulze, L., Bertram, A., Jansen, S., and Hamm, C. (2013). Size and biomechanical properties of diatom frustules influence food uptake by copepods. *Mar. Ecol. Prog. Ser.* 481, 41–51. doi: 10.3354/meps10227
- Gao, K., and Campbell, D. A. (2014). Photophysiological responses of marine diatoms to elevated CO₂ and decreased pH: A review. *Funct. Plant Biol.* 41, 449–459. doi: 10.1071/FP13247
- Giordano, M., Beardall, J., and Raven, J. A. (2005). CO₂ concentrating mechanisms in algae: mechanisms, environmental modulation, and evolution. *Annu. Rev. Plant Biol.* 56, 99–131. doi: 10.1146/annurev.arplant.56.032604.144052
- González-Dávila, M., Santana-Casiano, J. M., Rueda, M. J., and Llinás, O. (2010). The water column distribution of carbonate system variables at the ESTOC site from 1995 to 2004. *Biogeosciences* 7, 3067–3081. doi: 10.5194/bg-7-3067-2010
- Hamm, C., and Smetacek, V. (2007). “Armor: Why, when, and how,” in *Evolution of Phytoplankton*, eds P. G. Falkowski and A. H. Knoll (Boston, MA: Elsevier), 311–332.
- Hamm, C. E., Merkel, R., Springer, O., Jurkojc, P., Maiert, C., Prechtelt, K., et al. (2003). Architecture and material properties of diatom shells provide effective mechanical protection. *Nature* 421, 841–843. doi: 10.1038/nature01416
- Hansen, H. P., and Koroleff, F. (1999). “Determination of nutrients,” in *Methods of Seawater Analysis*, eds K. Grasshoff, K. Kremling, and M. Ehrhardt (Weinheim: Wiley-VCH), 159–226. doi: 10.1002/9783527613984.ch10
- Hervé, V., Derr, J., Douady, S., Quinet, M., Moisan, L., and Lopez, P. J. (2012). Multiparametric Analyses Reveal the pH-Dependence of Silicon Biomineralization in Diatoms. *PLoS One* 7:e46722. doi: 10.1371/journal.pone.0046722
- Hofmann, G. E., Smith, J. E., Johnson, K. S., Send, U., Levin, L. A., Micheli, F., et al. (2011). High-frequency dynamics of ocean pH: A multi-ecosystem comparison. *PLoS One* 6:e28983. doi: 10.1371/journal.pone.0028983
- Holmes, R. M., Aminot, A., Kérouel, R., Hooker, B. A., and Peterson, B. J. (1999). A simple and precise method for measuring ammonium in marine and freshwater ecosystems. *Can. J. Fish. Aquat. Sci.* 56, 1801–1808. doi: 10.1139/f99-128
- Hopkinson, B. M., Dupont, C. L., Allen, A. E., and Morel, F. M. M. (2011). Efficiency of the CO₂-concentrating mechanism of diatoms. *Proc. Natl. Acad. Sci. U. S. A.* 108, 3830–3837. doi: 10.1073/pnas.1018062108
- Hoppe, C. J. M., Hassler, C. S., Payne, C. D., Tortell, P. D., Rost, B. R., and Trimborn, S. (2013). Iron limitation modulates ocean acidification effects on Southern Ocean phytoplankton communities. *PLoS One* 8:e79890. doi: 10.1371/journal.pone.0079890
- Lavigne, H., Epitalon, J.-M., and Gattuso, J.-P. (2011). *Seacarb: seawater carbonate chemistry with R. R package version 3.0*. Available at: <http://cran.r-project.org/package=seacarb>
- Liu, H., Chen, M., Zhu, F., and Harrison, P. J. (2016). Effect of diatom silica content on copepod grazing, growth and reproduction. *Front. Mar. Sci.* 3:89. doi: 10.3389/fmars.2016.00089
- Lueker, T. J., Dickson, A. G., and Keeling, C. D. (2000). Ocean pCO₂ calculated from dissolved inorganic carbon, alkalinity, and equations for K₁ and K₂: Validation based on laboratory measurements of CO₂ in gas and seawater at equilibrium. *Mar. Chem.* 70, 105–119. doi: 10.1016/S0304-4203(00)00022-0
- Mann, D. G., and Vanormelingen, P. (2013). An Inordinate Fondness? The Number, Distributions, and Origins of Diatom Species. *J. Eukaryot. Microbiol.* 60, 414–420. doi: 10.1111/jeu.12047
- Martin-Jézéquel, V., Hildebrand, M., and Brzezinski, M. A. (2000). Review Silicon Metabolism in Diatoms: Implications for Growth. *J. Phycol.* 36, 821–840. doi: 10.1046/j.1529-8817.2000.00019.x
- McConville, K., Halsband, C., Fileman, E. S., Somerfield, P. J., Findlay, H. S., and Spicer, J. I. (2013). Effects of elevated CO₂ on the reproduction of two calanoid copepods. *Mar. Pollut. Bull.* 73, 428–434. doi: 10.1016/j.marpolbul.2013.02.010
- McGillicuddy, D. J., Anderson, L. A., Bates, N. R., Bibby, T., Buesseler, K. O., Carlson, C. A., et al. (2007). Eddy/Wind Interactions Stimulate Extraordinary Mid-Ocean Plankton Blooms. *Science* 316, 1021–1026. doi: 10.1126/science.1136256
- Mejía, L. M., Isensee, K., Méndez-Vicente, A., Pisonero, J., Shimizu, N., González, C., et al. (2013). B content and Si/C ratios from cultured diatoms (*Thalassiosira pseudonana* and *Thalassiosira weissflogii*): Relationship to seawater pH and diatom carbon acquisition. *Geochim. Cosmochim. Acta* 123, 322–337. doi: 10.1016/j.gca.2013.06.011
- Menden-Deuer, S., and Lessard, E. J. (2000). Carbon to volume relationships for dinoflagellates, diatoms, and other protist plankton. *Limnol. Oceanogr.* 45, 569–579. doi: 10.4319/lo.2000.45.3.0569
- Milligan, A. J., Varela, D. E., Brzezinski, M. A., and Morel, F. M. M. (2004). Dynamics of Silicon Metabolism and Silicon Isotopic Discrimination in a Marine Diatom as a Function of pCO₂. *Limnol. Oceanogr.* 49, 322–329. doi: 10.4319/lo.2004.49.2.0322
- Moreno de Castro, M., Schartau, M., and Wirtz, K. (2017). Potential sources of variability in mesocosm experiments on the response of phytoplankton to ocean acidification. *Biogeosciences* 14, 1883–1901. doi: 10.5194/bg-14-1883-2017
- Nelson, D. M., Tréguer, P., Brzezinski, M. A., Leynaert, A., and Quéguiner, B. (1995). Production and dissolution of biogenic silica in the ocean: Revised global estimates, comparison with regional data and relationship to biogenic sedimentation. *Global Biogeochem. Cycles* 9, 359–372. doi: 10.1029/95GB01070
- Oksanen, A. J., Blanchet, F. G., Friendly, M., Kindt, R., Legendre, P., Mcglinn, D., et al. (2018). *Package “vegan.” version 2.5-3*.

- Olenina, I., Hajdu, S., Edler, L., Wasmund, N., Busch, S., Göbel, J., et al. (2006). Biovolumes and size-classes of phytoplankton in the Baltic Sea. *HELCOM Balt. Sea Environ. Proc.* 106, 144.
- Pasciak, W. J., and Gavis, J. (1974). Transport limitation of nutrient uptake in phytoplankton. *Limnol. Oceanogr.* 19, 881–888. doi: 10.1016/j.cub.2014.12.004
- Paul, A. J., Bach, L. T., Schulz, K.-G., Boxhammer, T., Czerny, J., Achterberg, E. P., et al. (2015). Effect of elevated CO₂ on organic matter pools and fluxes in a summer Baltic Sea plankton community. *Biogeosciences* 12, 6181–6203. doi: 10.5194/bg-12-6181-2015
- Pondaven, P., Gallinari, M., Chollet, S., Bucciarelli, E., Sarthou, G., Schultes, S., et al. (2007). Grazing-induced Changes in Cell Wall Silicification in a Marine Diatom. *Protist* 158, 21–28. doi: 10.1016/j.protis.2006.09.002
- Reinfelder, J. R. (2011). Carbon concentrating mechanisms in eukaryotic marine phytoplankton. *Ann. Rev. Mar. Sci.* 3, 291–315. doi: 10.1146/annurev-marine-120709-142720
- Riebesell, U., Czerny, J., von Bröckel, K., Boxhammer, T., Büdenbender, J., Deckelnick, M., et al. (2013). Technical Note: A mobile sea-going mesocosm system – new opportunities for ocean change research. *Biogeosciences* 10, 1835–1847. doi: 10.5194/bg-10-1835-2013
- Rossoll, D., Bermúdez, R., Hauss, H., Schulz, K. G., Riebesell, U., Sommer, U., et al. (2012). Ocean acidification-induced food quality deterioration constrains trophic transfer. *PLoS One* 7:e34737. doi: 10.1371/journal.pone.0034737
- Rost, B., Riebesell, U., Burkhardt, S., and Sültemeyer, D. (2003). Carbon acquisition of bloom-forming marine phytoplankton. *Limnol. Oceanogr.* 48, 55–67. doi: 10.4319/lo.2003.48.1.0055
- Sarthou, G., Timmermans, K. R., Blain, S., and Tréguer, P. (2005). Growth physiology and fate of diatoms in the ocean: A review. *J. Sea Res.* 53, 25–42. doi: 10.1016/j.seares.2004.01.007
- Schulz, K. G., Bellerby, R. G. J., Brussaard, C. P. D., Büdenbender, J., Czerny, J., Engel, A., et al. (2013). Temporal biomass dynamics of an Arctic plankton bloom in response to increasing levels of atmospheric carbon dioxide. *Biogeosciences* 10, 161–180. doi: 10.5194/bg-10-161-2013
- Shen, C., and Hopkinson, B. M. (2015). Size scaling of extracellular carbonic anhydrase activity in centric marine diatoms. *J. Phycol.* 51, 255–263. doi: 10.1111/jpy.12269
- Sommer, U., Stibor, H., Katchakis, A., Sommer, F., and Hansen, T. (2002). Pelagic food web configurations at different levels of nutrient richness and their implications for the ratio fish production:primary production. *Hydrobiologia* 484, 11–20. doi: 10.1023/A:1021340601986
- Strickland, J. D. H., and Parsons, T. R. (1972). in *A practical handbook of seawater analysis*, ed. J. C. Stevenson Ottawa (Ottawa: Fisheries research board of Canada).
- Taucher, J., Aristegui, J., Bach, L. T., Guan, W., Montero, M. F., Nauendorf, A., et al. (2018). Response of Subtropical Phytoplankton Communities to Ocean Acidification Under Oligotrophic Conditions and During Nutrient Fertilization. *Front. Mar. Sci.* 5:330. doi: 10.3389/fmars.2018.00330
- Taucher, J., Bach, L. T., Boxhammer, T., Nauendorf, A., Achterberg, E. P., Algueró-Muñoz, M., et al. (2017). Influence of Ocean Acidification and Deep Water Upwelling on Oligotrophic Plankton Communities in the Subtropical North Atlantic: Insights from an In situ Mesocosm Study. *Front. Mar. Sci.* 4:85. doi: 10.3389/fmars.2017.00085
- Thor, P., Bailey, A., Dupont, S., Calosi, P., Søreide, J. E., De Wit, P., et al. (2018). Contrasting physiological responses to future ocean acidification among Arctic copepod populations. *Glob. Chang. Biol.* 24, e365–e377. doi: 10.1111/gcb.13870
- Tortell, P. D., Payne, C. D., Li, Y., Trimborn, S., Rost, B., Smith, W. O., et al. (2008). CO₂ sensitivity of Southern Ocean phytoplankton. *Geophys. Res. Lett.* 35, L04605. doi: 10.1029/2007GL032583
- Tréguer, P., Bowler, C., Moriceau, B., Dutkiewicz, S., Gehlen, M., Aumont, O., et al. (2018). Influence of diatom diversity on the ocean biological carbon pump. *Nat. Geosci.* 11, 27–37. doi: 10.1038/s41561-017-0028-x
- Tréguer, P. J., and De La Rocha, C. L. (2013). The World Ocean Silica Cycle. *Ann. Rev. Mar. Sci.* 5, 477–501. doi: 10.1146/annurev-marine-121211-172346
- Trimborn, S., Brenneis, T., Sweet, E., and Rost, B. (2013). Sensitivity of Antarctic phytoplankton species to ocean acidification: growth, carbon acquisition, and species interaction. *Limnol. Oceanogr.* 58, 997–1007. doi: 10.4319/lo.2013.58.3.0997
- Vrieling, E. G., Gieskes, W. W. C., and Beelen, T. P. M. (1999). Silicon deposition in diatoms: control by the pH inside the silicon deposition vesicle. *J. Phycol.* 35, 548–559. doi: 10.1046/j.1529-8817.1999.3530548.x
- Wallace, R. B., Baumann, H., Grear, J. S., Aller, R. C., and Gobler, C. J. (2014). Coastal ocean acidification: The other eutrophication problem. *Estuar. Coast. Shelf Sci.* 148, 1–13. doi: 10.1016/j.ecss.2014.05.027
- Welschmeyer, N. (1994). Fluorometric analysis of chlorophyll a in the presence of chlorophyll b and pheopigments. *Limnol. Oceanogr.* 39, 1985–1992. doi: 10.4319/lo.1994.39.8.1985
- Wilken, S., Hoffmann, B., Hersch, N., Kirchgessner, N., Dieluweit, S., Rubner, W., et al. (2011). Diatom frustules show increased mechanical strength and altered valve morphology under iron limitation. *Limnol. Oceanogr.* 56, 1399–1410. doi: 10.4319/lo.2011.56.4.1399
- Wolf-Gladrow, D., and Riebesell, U. (1997). Diffusion and reactions in the vicinity of plankton: A refined model for inorganic carbon transport. *Mar. Chem.* 59, 17–34. doi: 10.1016/S0304-4203(97)00069-8
- Wu, Y., Campbell, D. A., Irwin, A. J., Suggett, D. J., and Finkel, Z. V. (2014). Ocean acidification enhances the growth rate of larger diatoms. *Limnol. Oceanogr.* 59, 1027–1034. doi: 10.4319/lo.2014.59.3.1027
- Zhang, Y., Bach, L. T., Lohbeck, K. T., Schulz, K. G., Listmann, L., Klapper, R., et al. (2018). Population-specific responses in physiological rates of *Emiliania huxleyi* to a broad CO₂ range. *Biogeosciences* 15, 3691–3701. doi: 10.5194/bg-15-3691-2018

Conflict of Interest Statement: The authors declare that the research was conducted in the absence of any commercial or financial relationships that could be construed as a potential conflict of interest.

Copyright © 2019 Bach, Hernández-Hernández, Taucher, Spisla, Sforza, Riebesell and Aristegui. This is an open-access article distributed under the terms of the Creative Commons Attribution License (CC BY). The use, distribution or reproduction in other forums is permitted, provided the original author(s) and the copyright owner(s) are credited and that the original publication in this journal is cited, in accordance with accepted academic practice. No use, distribution or reproduction is permitted which does not comply with these terms.